

Hydrographic structure of the continental shelf in Santos Basin and its causes: The SANAGU and SANSED campaigns (2019)

Marcelo Dottori ¹*, Dalton K. Sasaki ¹, Danilo A. Silva ¹, Sergio R. Del-Giovannino ¹, Andressa P. Pinto ¹, Magnim Gnamah ¹, Arian D. Santos ¹, Ilson C. A. da Silveira ¹, Wellington C. Belo ², Renato P. Martins ² and Daniel L. Moreira ²

¹Oceanographic Institute, University of São Paulo, Praça do Oceanográfico, 191 São Paulo/SP 05508-120,

²Centro de Pesquisas, Desenvolvimento e Inovação Leopoldo Américo Miguez de Mello - CENPES/PETROBRAS, Av. Horácio Macedo, 950 - Cidade Universitária da Universidade Federal do Rio de Janeiro, Rio de Janeiro - RJ, 21941-915

*Corresponding author: mdottori@usp.br

ABSTRACT

This study describes the hydrography and water masses of the Santos Basin Continental Shelf (SBCS) during two hydrographic campaigns (SANAGU, SANSED) in 2019. Coastal Water (CW) is the dominant water mass in the southern portion of the SBCS, with relatively low salinity values ($S < 35.5 \text{ g kg}^{-1}$), and satellite data show that local precipitation and river discharge could not account for the low salinity observed during the cruises in the southern region of the domain. The low salinity observed is explained by the transport from the south influenced by Subtropical Shelf Water (STSW), which was influenced by the La Plata River discharge. In the northern region of the SBCS, the South Atlantic Central Water (SACW) dominates the bottom layers of the water column, with the wind playing a major role in the uplift of this water mass, as evidenced by a wind impulse analysis. In this part of the shelf, Tropical Water (TW) was the second water mass in volume and occupied the surface layers and offshore the shelf. CW is restricted to a thin surface layer, which reaches distances of a few kilometers from the coast. Our analysis shows the differences in the hydrographic structure of the SBCS and suggests that the SBCS can be divided in two regions with distinct characteristics: 1) the area southwest of São Sebastião, where the hydrographic parameters were modulated by the presence of the Subtropical Shelf Water (STSW); 2) the area northeast of São Sebastião, where the uplifting of SACW was the dominant process.

Keywords: Water Mass; Tropical Water; South Atlantic Central Water; Wind Impulse; Salinity; Continental Runoff

INTRODUCTION

The Santos Basin, or South Brazil Bight, Continental Shelf (hereafter SBCS – Figure 1) extends for approximately 1,100 km (Castro & Miranda 1998a), being located between Cabo Frio (23°S), in the

north, and Cabo de Santa Marta ($28^\circ 40'\text{S}$), in the south. The SBCS presents a relatively smooth topography and a shelf break depth varying between 120 and 180 meters (Castro & Miranda 1998b). It is wider in the central portion, around Santos (~ 230 km), and relatively narrow in the northern (~ 50 km) and southern (~ 70 km) limits. The Brazil Current (BC), a western boundary current of the South Atlantic, flows along the slope (Silveira et al. 2000)

Submitted: 31-May-2022

Approved: 4-January-2023

Associate Editor: Sílvia Sousa



© 2023 The authors. This is an open access article distributed under the terms of the Creative Commons license.

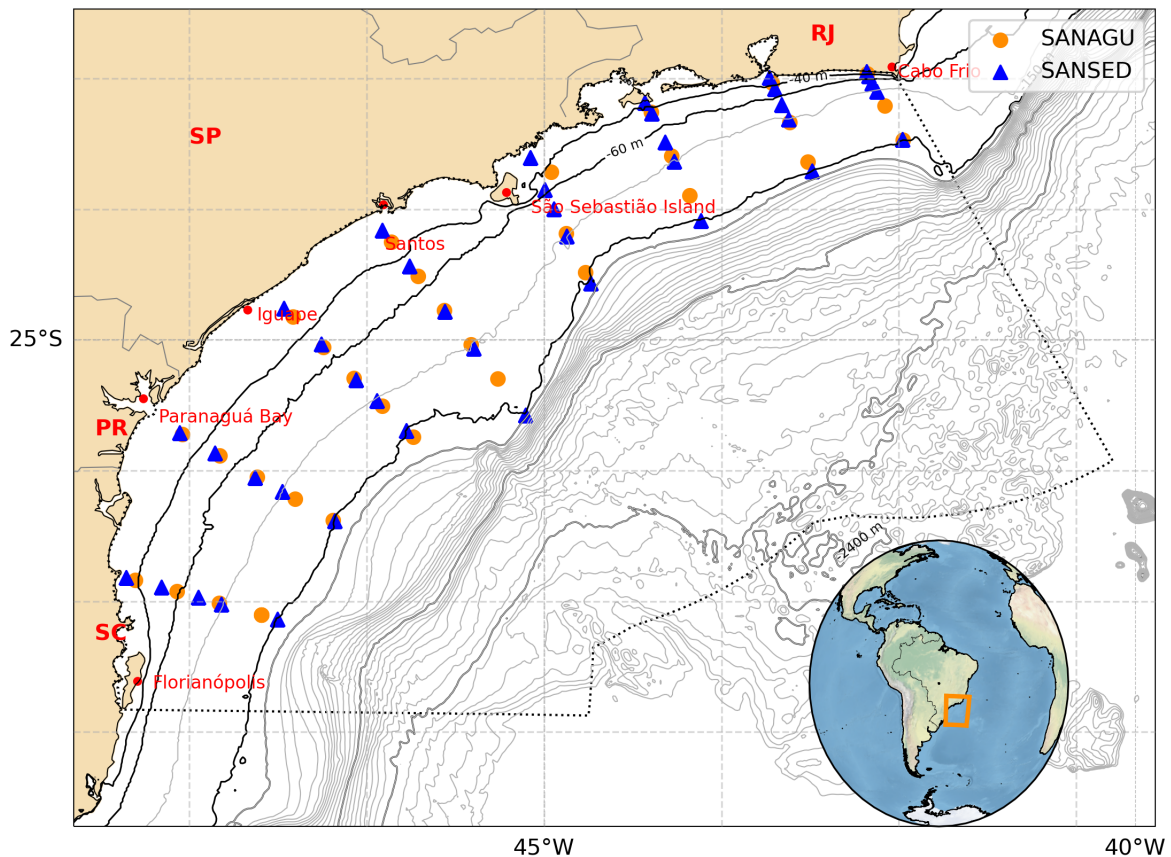


Figure 1. The Santos Basin Continental Shelf and its 40 m, 60 m and 200 m isobaths lines. The blue triangles show the SANSSED hydrographic stations and the orange circles, the SANAGU hydrographic stations. From southwest to northeast, the transects are named from A (off Santa Catarina State) to H (off Cabo Frio). From south to north are the states of Santa Catarina (SC), Paraná (PR), São Paulo (SP) and Rio de Janeiro (RJ).

and, therefore, the SBCS is classified dynamically as a “wide continental shelf with western boundary current at the shelf edge” (Loder et al. 1998).

The presence of several small rivers and two estuarine systems are responsible for discharging approximately $1,600 \text{ m}^3 \text{ s}^{-1}$ of freshwater, from Santa Catarina up to the São Sebastião Island (Marta-Almeida et al. 2021). Among these systems, the Cananéia–Iguape estuarine system is the main contributor (Mahiques et al. 2009), accounting for 60% of the total discharge in the region and is responsible for a low-salinity strip nearshore (Castro & Miranda 1998a). Some studies suggest that the La Plata river plume influences the SBCS, reaching the São Sebastião Island in extreme cases (Piola et al. 2005) or if persistent favorable winds occur

(Pimenta et al. 2005). In the region north of São Sebastião Island, the river contribution is relatively small, with the highest freshwater discharges occurring in summer (Cerdeira & Castro 2014). This freshwater input in the SBCS is responsible for the formation of Coastal Water (CW), a low salinity–high temperature water mass, when mixed with other two water masses present in the SBCS, the South Atlantic Central Water (SACW), characterized by low values of temperature (salinity of 35.2 and temperature of 13°C), and the warm and salty Tropical Water (TW) (salinity of 37.0 and temperature of 24°C) (Cerdeira & Castro 2014). Both TW and SACW are transported by the BC in the upper layer along the shelf break (Silveira et al. 2000). The transition between these water masses char-

acterize strong temperature and salinity gradients, creating ocean fronts. At the surface, the interface between CW and TW forms a salinity front, known as Superficial Haline Front (SHF), defined approximated by the 36–isohaline, while at the bottom the interface between CW and SACW forms a temperature front, so-called Bottom Thermal Front (BTF), whose location can be assumed as the 18 °C isotherm (Castro 2014). The average position of these fronts are used to divide the shelf into 3 portions off Ubatuba, but here we extend this division to the whole SBCS. The region between the coastline and the BTF is defined as the inner shelf and its width varies based on the BTF position: in summer, BTF is located between the 20 and 40 meters isobath (narrower), while in winter it is found between the 50 and 70 meters isobath (wider). The mid-shelf is located between the BTF and SHF, with an external limit found between the 70 m and 90 m isobaths. Finally, the outer shelf extends from the SHF up to the shelf break (Castro et al. 2008). Another water mass that eventually reaches the SBCS is the Subtropical Shelf Water (STSW), a water mass occurring between 33 °S and 28 °S, south of SBCS. Its salinity is strongly influenced by the runoff of the La Plata river, specially in winter when the 33 isohaline reaches 28 °S, while during summer it is limited to 32 °S (Piola et al. 2005). The temperature of STSW varies seasonally, from about 17 °C in winter, to 23 °C in summer (Piola et al. 2000).

The SBCS is under the influence of two meteorological systems. The South Atlantic Subtropical High (SASH) is the first one and is associated with upwelling–favorable and prevalent north-easterly winds, while the second is the transient synoptic cold fronts, which impose downwelling–favorable southwesterly winds, along with cold air incursions and increase in precipitation (Garreaud 2000). The SBCS is occasionally influenced by the presence of atmospheric blocking (Rodrigues & Woollings 2017), which affects the continental shelf dynamics (Silva & Dottori 2021). Based on the topographic and hydrographic characteristics, it is possible to divide the SBCS in two compartments taking the São Sebastião Island (Figure 1) as a geographical limit. The wider continental shelf corresponding to the southern compartment has

a greater influence of continental runoff (Marta-Almeida et al. 2021, Piola et al. 2000), and the narrow continental shelf in the northern compartment favors oceanic influence nearshore, while presenting a weaker influence of freshwater discharge (Cerdeira & Castro 2014). Hence, the dynamics of the southern SBCS are subject to wind and buoyancy flux action, while to the north, the dynamics is driven mainly by the winds (Morais 2016). Continental Shelf Waves (CSW) also play a role in the SBCS, presenting a faster propagation speed in the south ($\sim 10 \text{ m s}^{-1}$) when compared to the north ($\sim 7 \text{ m s}^{-1}$) (Dottori & Castro 2018). The entire SBCS presents a barotropic behavior that responds for 90% or more of the explained variance (Dottori & Castro 2009).

In this article, the thermohaline structure measured by comprehensive hydrographic surveys in 2019 over the entire SBCS is studied, considering the influence of STSW and upwelling–favorable winds. We present the hydrographic surveys and auxiliary datasets used in this analysis in the Methods section. The section Results are divided in two: we first describe the hydrographic conditions during the campaigns, and then present the processes influencing the thermohaline structure. We conclude this article with a discussion of all results, followed by a Concluding Remarks section with the main conclusions summarized.

METHODS

DATA SET

SANAGU and SANSED cruises were carried during the late winter and spring of 2019, the first one between August 8th and October 26th, and the second, from October 29th to November 23rd, as part of the Santos Project – Santos Basin Environmental Characterization – coordinated by PETROBRAS (Moreira et al. 2022 – this issue). This project had the intent of characterizing the Santos Basin in several aspects, including sampling of physical, biological, chemical and geological parameters. This long survey was performed onboard of R/V Seward Johnson. Temperature and salinity measurements, specifically, were taken with a CTD profiler probe (model SBE 911 plus) along transects with a trajec-

tory approximately perpendicular to the local isobaths (Figure 1). This study analyzes only the stations within the SBCS domain up to the shelf break (~ 200 m), although other stations were performed over the slope and deep ocean.

Salinity and temperature profiles were quality-controlled using a modified version of python-ctd software package (Fernandes 2014). These changes were minor adaptations of methods in python-ctd, which were necessary to circumvent peculiarities of the dataset. The spikes in the data were removed considering a 4 standard deviation threshold from the average, and the data was re-sampled at every meter. Finally, a 7-point window Hanning filter was employed to smooth the profiles.

Along with the *in-situ* data, three satellite products were selected for synoptic assessments: (1) absolute dynamic topography and geostrophic velocities of the Data Unification and Altimeter Combination System (DUACS) vDT2021, distributed by the Copernicus Marine Environment Monitoring Service; (2) sea surface temperature (SST) fields at 0.05° horizontal resolution based on daily, gap-filled fields of sea surface temperature (SST) from *in-situ* observations and also satellite data from the Operational Sea Surface Temperature and Sea Ice Analysis (OSTIA) (Stark et al. 2007, Donlon et al. 2012, Good et al. 2020); (3) gridded sea surface salinity fields from the Soil Moisture Active Passive ocean surface salinity v4.0 (SMAP-SSS) at 0.25° resolution, considering an 8-days running average (Meissner 2019). Finally, hourly winds from ERA reanalysis products 10 m above the sea surface were used, with 0.25° of horizontal resolution (Hersbach et al. 2020).

Conservative temperature and absolute salinity, which will be referred hereinafter as temperature and salinity only, are presented in Figure 2 and the values were calculated using the TEOS-10 equation of state (McDougall & Barker 2011). Hydrographic data (temperature and salinity) provided the fraction of the water masses based on the mixing triangle calculation (Mamayev 1975). Since the mixing processes in SBCS may involve three different water masses (CW, TW and SACW), the domain of a water mass is considered only when reached a 55% threshold minimum. In this work, the TS indices used to identify the water masses values

followed Cerda and Castro (2014) as $13^\circ\text{C} - 35.2$ for SACW and $24^\circ\text{C} - 37.0$ for TW. CW indices were determined by selecting the lowest salinity and associated temperature value in the upper 20 m of the water column at each transect.

The interpolation of stations onto transects is based on the Objective Analysis (OA) interpolation method (Bretherton et al. 1976, Carter & Robinson 1987). Objective Analysis consists of a method used to make systematic estimates from oceanographic observations and minimize the error of the estimates in a least-square sense (Bretherton et al. 1976). The optimal estimates were found by setting the horizontal correlation length of 160 km and 20 m in the vertical direction, while the measurement error used in the Gaussian covariance function was defined as 0.01. The horizontal correlation length was found by minimizing the error obtained by fitting an analytical gaussian curve to the position of each measurement, with a first guess being the order of the average barotropic deformation radius over the shelf ($O[100\text{ km}]$). The vertical correlation length of 0.3 m obtained from the fitting process was considered spurious, as it was a consequence of grouping the entire dataset positions. Instead, we select 20 m as the vertical length based on the average value of the mixed-layer depth in the innermost stations of the transects. Sensitivity analysis showed halving or doubling the values of correlation lengths and error do not change the general structure of the interpolated fields. Only stations considered synoptic were used to build the interpolated cross-sections (Figure 1), meaning that the time between the first and last station did not exceed 5 days.

Coastal upwelling/uplifting of SACW in the northern portion of the domain can be associated to the wind regime (Csanady 1977). In this region, negative values of wind impulse favor the isopycnal uplift in SBCS, with the wind impulse (I) given by:

$$I = \int_0^T \frac{\tau_y}{\rho} dt \quad (1)$$

where τ_y is the alongshore wind stress component, ρ is the mean water density (assumed here as 1025 kg m^{-3}) and T is the period of wind action. The wind stress is parameterized through the bulk aerodynamic relation:

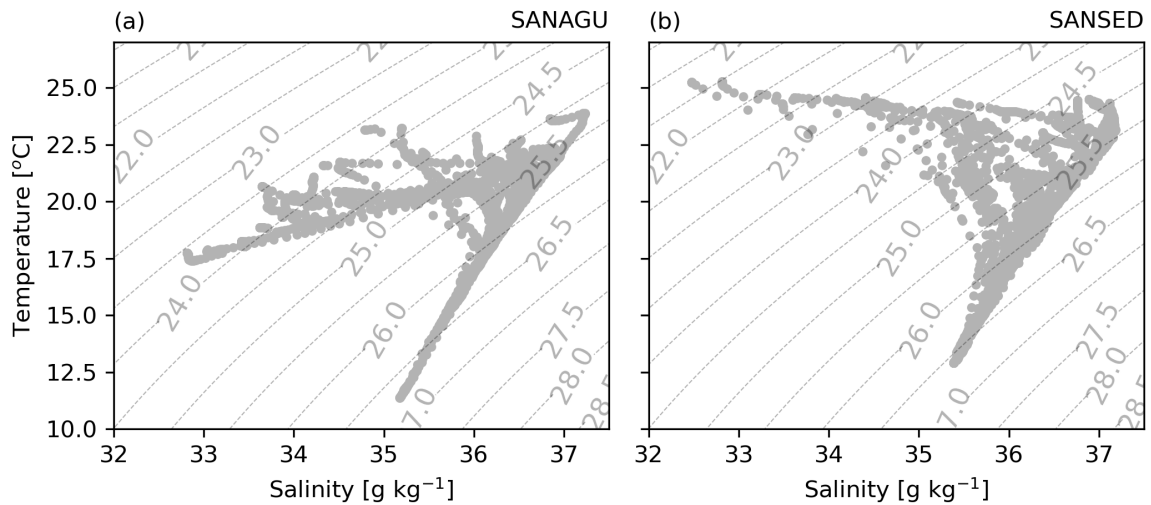


Figure 2. TS diagrams obtained for all the hydrographic stations. The left panel presents the SANAGU campaign and the right panel, the SANSED campaign. The values presented are the conservative temperature and the absolute salinity obtained with TEOS–10 equation of state (McDougall & Barker 2011).

$$\tau_y = \rho_{air} C_D v_{10} |\bar{w}_{10}| \quad (2)$$

where ρ_{air} is the air density (1.225 kg m^{-3}), C_D is the drag coefficient (0.0015), \bar{w}_{10} is the 10-m wind horizontal velocity and v_{10} is its alongshore component, both 10 m above the sea level. The alongshore component of the wind vector was obtained considering that the orientation of the local coastline is rotated 45° clockwise from the real north. The wind impulse was calculated using the average wind stress over the corresponding transect. We used hourly wind time series from ERA5 reanalysis, between August and December 2019.

RESULTS

HYDROGRAPHY

Hydrographic transects are identified as A, B, C and D, in the southern part of the domain, and E, F, G, and H, in the northern portion (Figure 1). Figure 2 presents the TS diagram of all measured vertical profiles on the shelf. Two distinct hydrographic conditions were observed from the TS pairs, considering pairs with values of sigma density (hereafter only density) lower than 25 kg m^{-3} . It shows the CW associated temperatures were usually colder

($\sim 5^\circ\text{C}$) during SANAGU.

During the SANAGU campaign (Figure 2 a), the SBCS hydrographic environment presented typical conditions of winter (Castro 2014). In the southern portion (transects A to D—Figure 1), TW prevented the mixing between the CW and the SACW, even though a large volume of CW was observed (Figure 3). In this case, water mixing occurred only in TW/SACW and TW/CW interfaces. It is clear in the TS diagrams of these transects that CW was separated from SACW by an intermediate layer of TW. Waters with low salinity ($< 35 \text{ g kg}^{-1}$) usually present higher temperatures ($> 20^\circ\text{C}$) in typical summer conditions (Figure 2 b).

The normalized area percentage of water masses (hereinafter area percentage) shows the contribution of each water mass to each transect considering the inner and mid-shelf (Figure 4). The area percentage is the ratio between the area occupied by a given water mass and the selected sectional area in a given transect. The selected sectional area is defined as the rectangle in the upper 100 m of the water column with a width of 80 km starting from the shallowest station. Two main patterns are present: (1) CW dominates the inner and mid-shelf in southern SBCS (Figure 4); (2) SACW is dominant in the northern SBCS, where

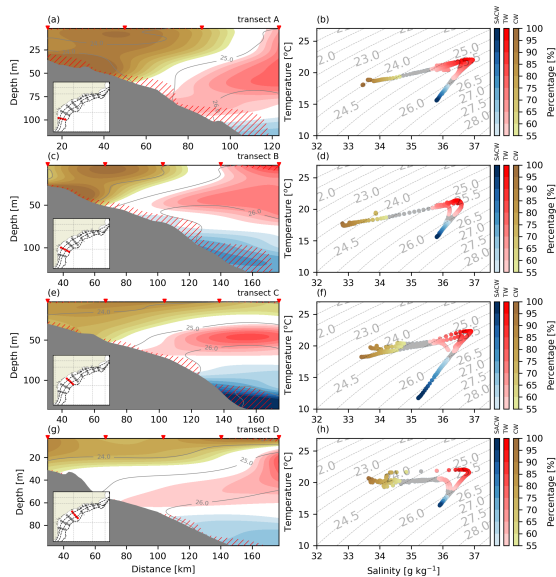


Figure 3. Sections of water mass (a, c, e, g) and the corresponding TS diagrams (b, d, f, h) at the southern part of the domain (transects A to D) during the SANAGU cruise. The yellow dots on the map (Figure 1) and red triangles over the panels on the left indicate the concomitant position of CTD stations. The colors of the TS diagrams follow the water mass percentage indicated in the color bar. The red hatched areas indicate the region where the interpolation error is above 5%. Also, the white color region on the left and gray colors on the right panels indicate a water mix with no dominant water mass.

it occupied more than 35% of the transect area in all cases.

Interpolated transects of CW, TW, and SACW percentages are presented in Figures 3, 5, 6 and 7. Temperature and salinity transects are presented as supplemental material (<https://zenodo.org/record/7507716#.Y7hKBqfMJy1>).

During SANAGU, CW occupied large portions of the continental shelf, reaching depths up to 50 m in transect A (Figure 3). In transect B to D, CW progressively spreaded to the upper 20 m towards the open ocean, with the lower limit isopycnals tilted to the surface and TW occupying increasing areas (although <15% of the area) (Figure 4). SACW was restricted to relatively deep areas (>60 m) in the southern SANAGU transects (Figure 3). This fact explains the absence of its signal in Figure 4, since the sectional area used to calculate the percent-

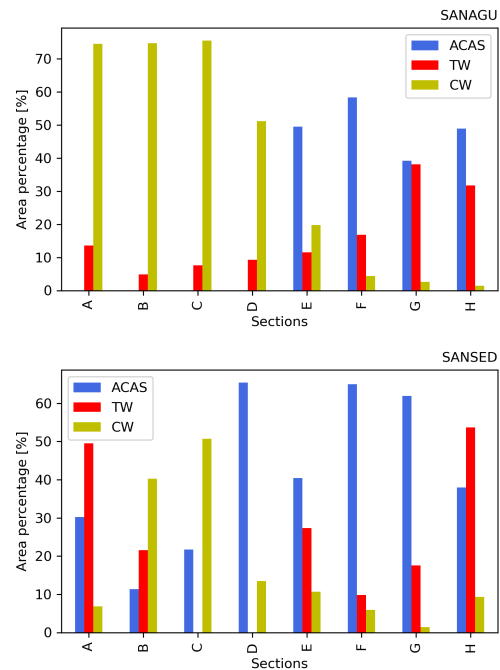


Figure 4. Fraction (%) of the area occupied by each water mass in SANAGU (top panel) and SANSÉD (bottom panel) sections, considering a fixed area. The area is defined as the upper 100 m and first 80 km from the closest station to the coast. Regions with interpolation error greater than 5% were not included.

age did not include the regions where SACW was present. Salinity associated with CW in the area was typically lower than 34.5 g kg^{-1} , while temperature ranged from $17 \text{ }^{\circ}\text{C}$ to $22 \text{ }^{\circ}\text{C}$. The maximum depth of CW at transect D was about 40 m.

In SANSÉD, the CW was restricted to the upper 30 m and presented higher ranges of temperature values ($20.0 \text{ }^{\circ}\text{C}$ to $25.0 \text{ }^{\circ}\text{C}$), with a maximum salinity value of about 35.5 g kg^{-1} . The signal of CW was associated with the coast, but in transect C the core of the water mass was centered 80 km offshore, while close to the coast mixed waters were dominant (Figure 5). In transect D, a blob of CW is located mainly at the outer shelf, where it also presented lower limits at about 25 m depth, while in the inner and mid-shelf CW occupied the upper 5 m of the water column only. Since the CW in SANSÉD did not occupy the entire inner and mid-shelf, TW and SACW were present in the remaining areas. In SANSÉD, only transect A and B presented TW and

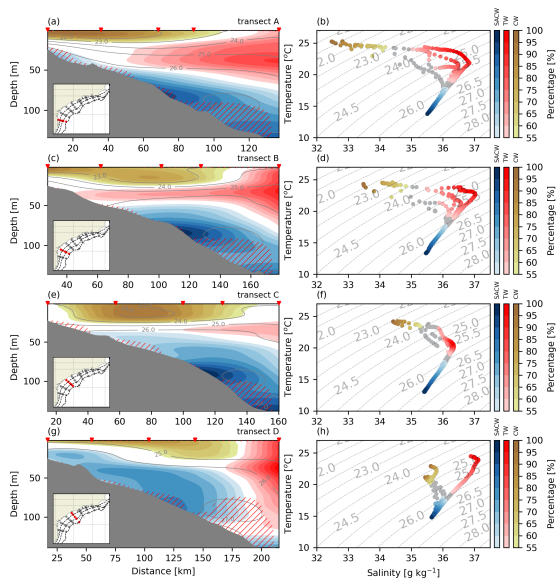


Figure 5. Sections of water mass (a, c, e, g) and the corresponding TS diagrams (b, d, f, h) at the southern part of the domain (transects A to D) during the SANSED cruise. The blue triangles on the map (Figure 1) and red triangles over the panels on the left indicate the concomitant position of CTD stations. The colors of the TS diagrams follow the water mass percentage indicated in the color bar. The red hatched areas indicate the region where the interpolation error is above 5%. Also, the white color region on the left and gray colors on the right panels indicate a water mix with no dominant water mass.

SACW in the inner and mid-shelf, while transects C e D showed only SACW and CW (Figure 4). In these transects, SACW was present at shallower depths relative to SANAGU, with its upper limit ranging from approximately 10 m in transect D to 50 m in transect B. These cases presented shoreward isopycnals related to SACW occupying large areas (>30%) of the inner and mid-shelf, which explains their presence in transects A to D (Figure 4).

SANSED shows a more stratified environment relative to SANAGU, where CW generally dominated the inner and mid-shelf. In transects A and B of SANAGU, TW was present only at the surface and on the outer shelf, whereas in transects C and D it only occurred at subsurface levels. During this cruise, TW was in contact with the bottom at depths of about 60 m. In the South Atlantic, TW usually occupies the top layer of the water column at deep

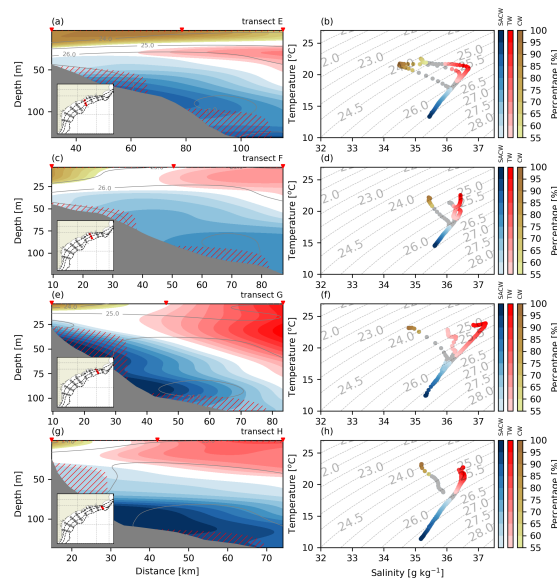


Figure 6. Sections of water mass (a, c, e, g) and the corresponding TS diagrams (b, d, f, h) at the northern part of the domain (transects E to H) during the SANAGU cruise. The yellow dots on the map (Figure 1) and red triangles over the panels on the left indicate the concomitant position of CTD stations. The colors of the TS diagrams follow the water mass percentage indicated in the color bar. The red hatched areas indicate the region where the interpolation error is above 5%. Also, the white color region on the left and gray colors on the right panels indicate a water mix with no dominant water mass.

waters (Valla et al. 2018), but on the shelf it was registered at subsurface levels in between the CW and SACW and with density ranging from 25.0 kg m^{-3} to 26.0 kg m^{-3} (Figures 3 and 6). During SANSED, TW was present at the surface in all transects with exception of transect C, with a characteristic isopycnal of 25.5 kg m^{-3} . In this cruise, TW was in contact with the ocean floor only in transect B at a depth of about 40 m.

In the southern region, the difference of stratification between the SANAGU and SANSED cruises considering the inner and mid-shelf is evident: SANAGU waters showed density values ranging from 21.5 kg m^{-3} (CW) to over 26.0 kg m^{-3} (SACW), while the density values in SANSED ranged from $\sim 24.5 \text{ kg m}^{-3}$ to 26.0 kg m^{-3} . These ranges reinforce the role of CW in the stratification of the southern shelf, where greater volumes of

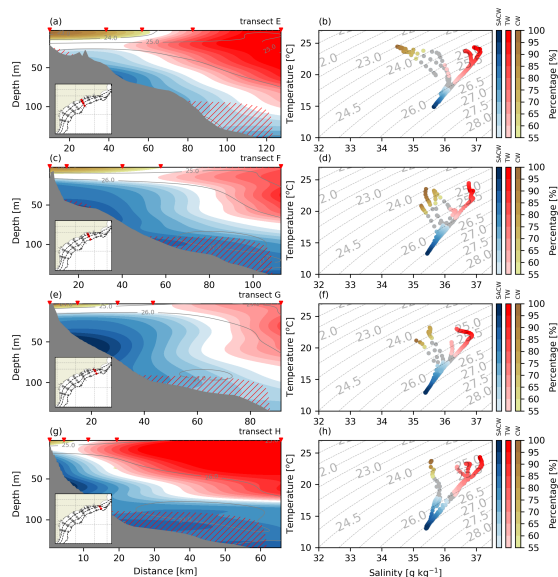


Figure 7. Sections of water mass (a, c, e, g) and the corresponding TS diagrams (b, d, f, h) at the northern part of the domain (transects E to H) during the SANSED cruise. The blue triangles on the map (Figure 1) and red triangles over the panels on the left indicate the concomitant position of CTD stations. The colors of the TS diagrams follow the water mass percentage indicated in the color bar. The red hatched areas indicate the region where the interpolation error is above 5%. Also, the white color on the left and gray colors on the right panels indicate a water mix with no dominant water mass.

lower salinity waters seem to inhibit the presence of TW and SACW.

As mentioned earlier, the northern SBCS presents a thermohaline structure different from the southern SBCS, with SACW dominant the thermohaline structure. In the inner and mid-shelf, SACW was often found between the ocean floor and depths up to 20 m to 30 m, usually occupying almost the entire water column. The area percentage occupied by SACW in the northern transects is on the average 10% higher in SANSED than in SANAGU. The sectional area of CW in the northern transects generally presented smaller volumes than their southern counterparts in both cruises. For instance, the maximum area percentage values related to CW in SANSED was about 10% ($\sim 50\%$) in the northern (southern) domain, while SANAGU showed maximum values of about 20% ($\sim 75\%$) in the north (south) (Figure 4). In the northern tran-

sects, CW was restricted to the upper 20 m and reached a maximum distance of 60 km offshore. In the northern SBCS, TW presented greater percentages ($\sim 10\%$ to $\sim 35\%$) of the sectional area when compared to the southern SBCS ($\sim 5\%$ to $\sim 12\%$) in SANAGU cruise. In SANSED, the area percentage of TW does not show patterns which can be differentiated in terms of northern and southern domain, as CW showed. In the northern domain, TW did not reach the ocean floor and its closest distance to the coastline was about 30 km (Figures 6 and 7).

PROCESSES INFLUENCING THE WATER MASS STRUCTURE ON THE SHELF

As previously shown, the northern SBCS is mainly influenced by the presence of SACW, while the southern domain contained large volumes of CW. The continental shelf waters showed a winter-like TS structure (lack of mixing between SACW and CW) during the SANAGU campaign, while the later cruises in SANSED presented a summer-like TS structure (mixing between the three water masses). This section, therefore, analyzes the environmental conditions that led to the observed hydrographic structure by evaluating satellite fields of salinity, temperature and precipitation, south of São Sebastião Island, and the wind impulse based on wind time series from the global reanalysis ERA5 (Hersbach et al. 2020) in the northern section.

The evolution of surface salinity and temperature fields using satellite data at selected dates is presented in Figure 8 and can indicate the remote source of low salinity waters. Close to the coast, the temperature fields of OSTIA have a better resolution than SMAP salinity data and are useful as a proxy to track the water advection along the coast. In the map, the southwestern boundaries are extended beyond the SBCS limits, since the surface temperature and salinity presented values corresponding to the Sub Tropical Surface Water (STSW) and were advected to the SBCS. This advection occurred as a pulse of water, influencing both surface salinity and temperature fields for the SANAGU campaign. In our analysis, the pulse started on August 12th, with waters of relatively low values of temperature ($T < 16^\circ\text{C}$) and salinity ($S < 31\text{ g kg}^{-1}$) to the south of 28.5°S (Figure 8 a,d). These waters advanced

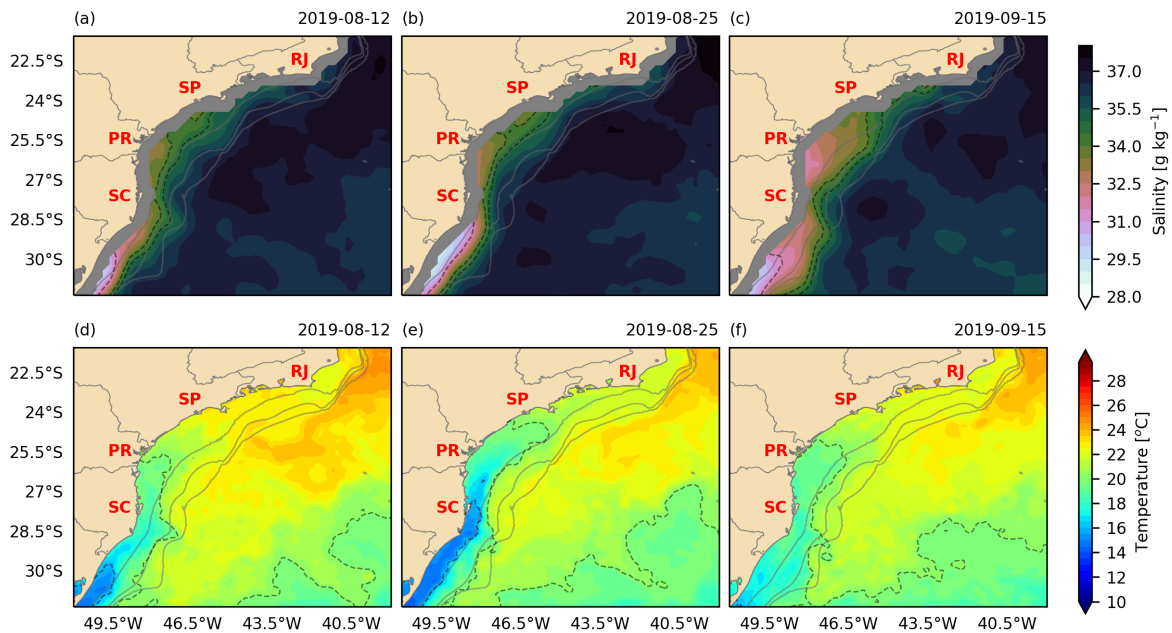


Figure 8. Surface maps of salinity (a, b, c) and temperature (d, e, f) show the evolution of fields during SANAGU cruise. Gray contours represent the 100, 200 and 1000 m isobaths and black dashed contours represent the 31.5, 34.0 and 34.8 g kg^{-1} isohalines and 16 and 20 $^{\circ}\text{C}$ isotherms. Gray color in the map background represents areas with no valid data. From south to north are the states of Santa Catarina (SC), Paraná (PR), São Paulo (SP) and Rio de Janeiro (RJ).

northward along the shelf and reached the northern boundary of Santa Catarina state (SC) on August 25th (Figure 8 b,e). On September 15th, the temperature values on the shelf along the coast of SC and Paraná states (PR) increased to $\sim 18^{\circ}\text{C}$, while the salinity showed decreased values on the shelf along São Paulo state (SP) (Figure 8 c,f). The STSW pulse was a consequence of a transient elevation of the sea surface height in August, which supported northward geostrophic ($O[10^{-1} \text{ m s}^{-1}]$) currents along the coast and the injection of STSW to the SBCS domain (Figure 9). Notice that the DUACS product can reproduce coastal monthly sea level variability reasonably well in the region (Etcheverry et al. 2015). A similar equatorward injection is present in the OSTIA temperature fields during the first two weeks of July (not shown), when values dropped from about 23°C along SC coast to approximately 21°C . This injection is compatible with average absolute dynamic topography in July, which presented a shoreward gradient in the coast from Uruguai to Santa Catarina. Unfortunately, SMAP measurements were unavailable dur-

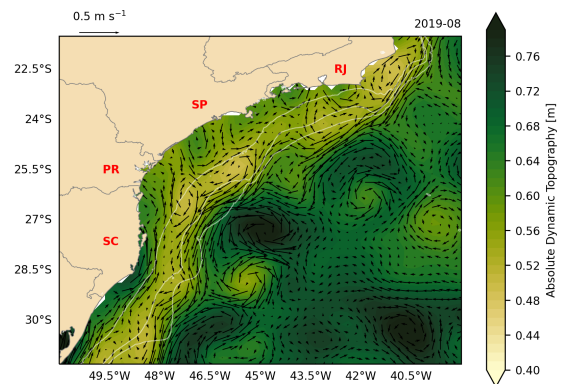


Figure 9. Average absolute dynamic topography from DUACS of August 2019 and associated geostrophic velocities (vectors). White contours correspond to 100, 200 and 1000 m isobaths.

ing this period.

The STSW signal is also present in the time series of salinity and temperature spatial averages in two regions along South America's coast (Figures 10 and 11). The time series shows a negative trend in the average salinity from 34 g kg^{-1} to 31.5 g kg^{-1}

in August on the shelf along Rio Grande do Sul state (Figure 10 a). These values are influenced by the presence of the STSW and also affected the waters along the SBCS, where salinity dropped from approximately 34.8 g kg^{-1} to 33.0 g kg^{-1} from August to mid-September (Figure 11 a). To the south, the average temperature time series shows waters from a domain corresponding to the inner shelf and slope, where the low temperature is a consequence of the northward along shelf pulse of STSW (Figure 11 c). The area used to calculate the time series of temperature to the south of the São Paulo coast did not capture the minimum signal of temperature in SBCS (Figure 11 c), which was constrained to the south of 26°S with relatively constant values ($\sim 20.0^\circ\text{C}$) until October. After August 25^{th} , the STSW signal started to be eroded by mixing and/or air–sea interaction processes, probably (Figure 10 a, c). On September 15^{th} , the original signature of STSW temperature was absent in the OSTIA SST fields, while surface salinity showed minimum values on the shelf along the coast of São Paulo state (Figure 8 a). The precipitation time series from both regions (Figures 10 b and 11 b) suggest that there is no direct relation between precipitation and salinity variability (Figures 10 a and 11 a), considering that the lowest salinity values are not coincident with the precipitation peaks.

The variability of SACW along the shelf may be explained partially by the wind forcing. Figure 12 presents the wind impulse time series calculated over transects D and G (Figure 1) in SANAGU and SANSED campaigns. In both time series, the wind impulse shows a negative trend, which represents an overall prevalence of northeasterly upwelling–favorable winds in the domain. An interval of 67 days separates the start and end of transect D measurements in SANAGU and the final measurement of the same transect in SANSED. During this period the wind impulse ($-240 \text{ m}^2 \text{ s}^{-1}$) contributed to the uplift of SACW from 70 m depth in the mid–shelf to about 10 m in the inner shelf. On the other hand, the interval between initial (SANAGU) and final measurement (SANSED) of transect G spanned 5 days. The upwelling–favorable impulse corresponding to this period was approximately $-18 \text{ m}^2 \text{ s}^{-1}$. The wind impulse during or prior in sections D and G of both cruises indicates a favorable environment for the

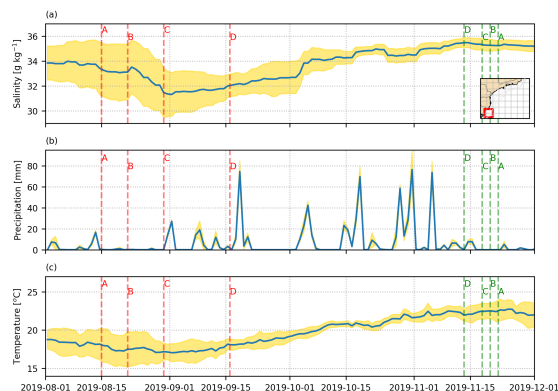


Figure 10. Time series of (a) salinity, (b) precipitation and (c) temperature calculated from the spatial average based on the red rectangle in the map, for the Rio Grande do Sul shelf. Dashed lines indicate the average date of each transect, with red (green) representing SANAGU (SANSED) transects. The yellow shaded region indicates the standard deviation from the spatial mean.

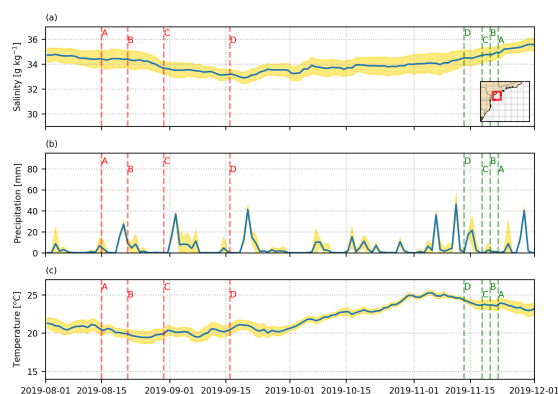


Figure 11. Time series of (a) salinity, (b) precipitation and (c) temperature calculated from the spatial average based on the red rectangle in the map, for the south area of the São Paulo coast. Dashed lines indicate the average date of each transect, with red (green) representing SANAGU (SANSED) transects. The yellow shaded region indicates the standard deviation from the spatial mean.

coastal upwelling of SACW, resulting in the uplift of the observed isopycnals (26 kg m^{-3} isopycnal) and a SACW–dominating bottom (Figures 6 and 7, panels e and g).

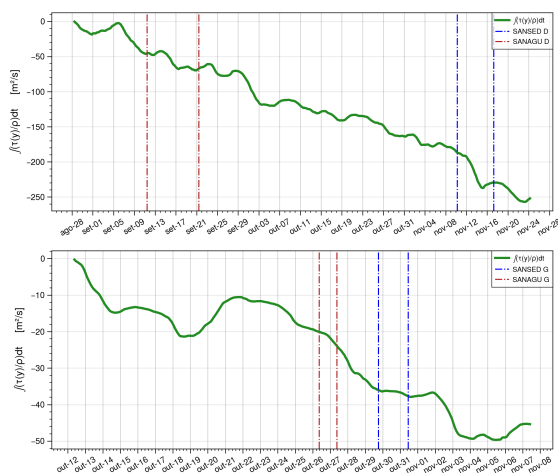


Figure 12. Time series of wind impulse (in green) averaged over the area traversed by the cruises in transects D (panel a) and G (panel b) that indicate a favorable environment for the uplift of the SACW. Vertical lines show the start and end of SANSSED (blue) and SANAGU (red) surveys at transects D and G.

DISCUSSION

The SANAGU and SANSSED campaigns represented major sampling efforts across the entire SBCS, from Santa Catarina, in the south, to Cabo Frio, in the north (Figure 1). The SANAGU campaign presented a winter-like TS diagram (Figure 2) similar to what was reported in other studies (Castro 2014). This structure illustrates the absence (or reduced occurrence) of SACW and CW mixing, which are usually separated by the presence of TW at intermediate levels. This disconnection between CW and SACW, however, is mainly observed south of São Sebastião Island (Figure 3), where there is a higher CW volume relative to the north.

During the SANAGU campaign, the contact between TW and the ocean floor in the southern domain contrasted with SANSSED cases, when TW was usually underneath CW. High CW volumes during SANAGU were influenced by the injection of the colder and fresher STSW into SBCS during July and August, identified mainly by the SST fields up to 26 °S. Apparently, local sources of freshwater – either precipitation over the ocean or river discharge – did not play an evident role in the salinity fields. Our combined analysis of satellite measurements of temperature, salinity and absolute dynamic to-

pography demonstrated the equatorward pulses of STSW were a consequence of a transient elevation in the sea surface height and its associated northward alongshore geostrophic currents south of 27 °S. In the region, these are known to be associated to the winds and/or trapped coastal waves (Castro & Lee 1995, Möller Jr et al. 2008). The advection of low salinity waters may be a seasonal response, but unfortunately the short time span of SMAP (about 7 years) does not allow to assess the signal significance. Interannual variability on the precipitation and associated river discharge are unlikely to play a role in the STSW advection, since increased discharge values usually associated with El Niño are important to northeastward injections only when the winds are favorable (Piola et al. 2005). After September, salinity values increased as local rivers and precipitation were not able to maintain the low salinity values.

It is important to note that in the southernmost part of the domain, the remote CW presence can last for relatively long periods. For instance, the SANAGU campaign sampled the continental shelf transects A to C between August 14th (start of transect A) and August 29th (end of transect C) and in SANSSED campaign, between November 11th (start of transect C) and November 23rd (end of transect A) (Figures 3 and 5). Therefore, the large amount of remote CW was not completely eroded after 3 months, at least. Therefore, when anomalous conditions like this are observed, the possible sources of CW in this specific region can be related not only to a remote source, but also lagged in time, since it can persist for an entire season. Even at transect D, located near at the middle of the domain, SANAGU (between 11th and 21st of September) and SANSSED (between 15th and 17th of November) campaigns show that this remote CW lasts for long periods of time.

In SANSSED, the SBCS presented summer-like conditions, similar to those observed by Castro (2014). During SANSSED and SANAGU, SACW occupied more than 50% of the water volume in the inner and mid-shelf of the northern transects. This relatively high amount of SACW occurs frequently at the northern domain of the SBCS, with winds from north-northeast as the main driving mechanism and commonly observed during spring/summer

months (Campos et al. 2000, Castro 2014, Cerda & Castro 2014), as it was the case for SANSED and SANAGU campaigns. The northern part of the SBCS is relatively narrow, favoring the influence of oceanic water masses (Silveira et al. 2000) and upwelling processes. Transect G shows that the hydrographic structure can change relatively fast, as the uplift of the isopycnal likely associated to the wind impulse ($-18 \text{ m}^2 \text{ s}^{-1}$) above the 60 m isobath from 50 m to 10 m depth occurred in a short period (5 days). For this transect, SANAGU (between 26th and 27th of October) and SANSED (between 29th and 31st of October) samplings were taken only few days apart, showing that the wind can modify the water masses structure in subinertial time scale (Figures 6 and 7). A remarkable uplift of SACW in transect D from 70 m in the mid-shelf to 10 m in the inner shelf from September 11th to November 16th (Figures 6 and 7) illustrates the difficulties of a coastal upwelling to occur along the São Paulo state coast. The uplift across this wide continental shelf (200 km) did not present a surface outcrop of SACW even after a period of strong upwelling–favorable wind impulse ($-240 \text{ m}^2 \text{ s}^{-1}$). For instance, the narrow shelf ($\leq 100 \text{ km}$) to the north of SBCS presented upwelling events after a wind impulse of only $-64 \text{ m}^2 \text{ s}^{-1}$, even though the slope dynamics could play a role (Palóczy et al. 2014, Calado et al. 2010). During SANAGU and SANSED surveys, the uplift of SACW at the shelf was certainly influenced by the cross shelf transport related to the wind impulse dynamics, but a subsurface along shelf transport of SACW originating from the coast along RJ might also be important (Cerda & Castro 2014). The other transects in the northern portion of the domain (F and H) were sampled with a delay of about 1 month, and, therefore, subinertial changes are not possible to observe, although they may occur.

CONCLUDING REMARKS

In this paper, the evaluation of the water mass distribution on the SBCS shelf during the SANAGU and SANSED campaigns in 2019 is provided along with the analysis of the environmental conditions responsible for the observed hydrographic structures. SANAGU cruise measurements were made from August to late October, while SANSED measure-

ments occurred from late October to late November. The continental shelf was classified in two regions to the north and south of São Sebastião Island. The water mass structure was controlled in the north and in the south, respectively, by the uplifting of the SACW and the modulation of temperature and salinity fields due to the influence of STSW on the shelf. The STSW was important over the SANAGU period, when the transects presented typical winter characteristics, with colder and fresher waters in the southern domain occupying large portions of the inner and mid-shelf. By November, the STSW was not completely eroded, with CW and TW occupying, respectively, the upper and bottom layer of the water column in the inner and mid-shelf. The observed uplifting of SACW over the northern domain in the period between SANAGU and SANSED is a consequence of the wind forcing, which was upwelling favorable. Therefore, as a major conclusion, the south domain hydrographic structure was mainly dominated by remote buoyancy forcing, very likely water from the La Plata river, while the north domain was wind-driven with uplifting of SACW dominating the bottom of the shelf.

ACKNOWLEDGMENTS

We thank Petróleo Brasileiro S.A. (PETROBRAS) for their permission to use and display the proprietary data from Santos Project – Santos Basin Environmental Characterization – for this paper. This study makes use of datasets provided by the E.U. Copernicus Marine Service Information, the Physical Oceanography Distributed Active Archive Center (PO.DAAC), the Copernicus Climate Change Service information, and the Centro de Previsão de Tempo e Estudos Climáticos (CPTEC/INPE). The authors would like to thank all these organizations for making the dataset available. The results contain modified Copernicus Climate Change Service information 2022. Neither the European Commission nor ECMWF is responsible for any use that may be made of the Copernicus information or data it contains. SMAP salinity data are produced by Remote Sensing Systems and sponsored by the NASA Ocean Salinity Science Team. They are available at www.remss.com. We also thank the reviewers for their valuable suggestions and comments, which

considerably improved the quality of this article.

AUTHOR CONTRIBUTIONS

M.D.: Conceptualization; Formal analysis; Funding acquisition; Investigation; Methodology; Project administration; Writing – original draft; Writing – review & editing;

D.K.S., D.A.S.: Data curation; Formal analysis; Methodology; Supervision; Writing – original draft; Writing – review & editing;

S.R.D.G., A.P.P., M.G., A.D.S.: Data curation; Formal analysis; Writing – original draft;

I.C.A.S.: Conceptualization; Funding acquisition; Investigation; Writing – original draft; Writing – review & editing;

W.C.B., R.P.M., D.L.M.: Funding acquisition; Investigation; Writing – review & editing.

REFERENCES

- BRETHERTON, F. P., DAVIS, R. E. & FANDRY, C. 1976. A technique for objective analysis and design of oceanographic experiments applied to mode-73, *Deep Sea Research and Oceanographic Abstracts*, Vol. 23, Elsevier, pp. 559–582.
- CALADO, L., DA SILVEIRA, I., GANGOPADHYAY, A. & DE CASTRO, B. 2010. Eddy-induced upwelling off cape São Tomé (22°S, Brazil), *Continental Shelf Research* **30**(10-11): 1181–1188.
- CAMPOS, E. J. D., VELHOTE, D. & DA SILVEIRA, I. C. A. 2000. Shelf break upwelling driven by Brazil Current cyclonic meanders, *Geophysical Research Letters* **27**: 751–754.
- CARTER, E. F. & ROBINSON, A. R. 1987. Analysis models for the estimation of oceanic fields, *Journal of Atmospheric and Oceanic Technology* **4**(1): 49–74.
- CASTRO, B. D. & MIRANDA, L. D. 1998a. Physical oceanography of the western Atlantic continental shelf located between 4° N and 34° S, *The Sea* **11**(1): 209–251.
- CASTRO, B. & MIRANDA, L. 1998b. Hydrographic properties in the São Sebastião channel: Daily variations observed in March, 1980, *Revista Brasileira de Oceanografia* **46**(2): 111–123.
- CASTRO, B. M. 2014. Summer/winter stratification variability in the central part of the South Brazil Bight, *Continental Shelf Research* **89**: 15–23.
- CASTRO, B. M. & LEE, T. N. 1995. Wind-forced sea level variability on the southeast Brazilian shelf, *J. Geophys. Res.* **100**(C8): 16,045–16,056.
- CASTRO, B. M., MIRANDA, L. B., SILVA, L. S., FONTES, R. F. C. ., PEREIRA, A. F. & COELHO, A. L. 2008. *Processos físicos: Hidrografia, circulação e transporte*, EDUSP.
- CERDA, C. & CASTRO, B. M. 2014. Hydrographic climatology of South Brazil Bight shelf waters between Sao Sebastiao (24°S) and Cabo Sao Tome (22°S), *Continental Shelf Research* **89**: 5–14.
- CSANADY, G. 1977. Intermittent ‘full’ upwelling in Lake Ontario, *Journal of Geophysical Research* **82**(3): 397–419.
- DONLON, C. J., MARTIN, M., STARK, J., ROBERTS-JONES, J., FIEDLER, E. & WIMMER, W. 2012. The operational sea surface temperature and sea ice analysis (OSTIA) system, *Remote Sensing of Environment* **116**: 140–158.
- DOTTORI, M. & CASTRO, B. M. 2009. The response of the São Paulo continental shelf, Brazil, to synoptic winds, *Ocean Dynamics* **59**(4): 603–614.
- DOTTORI, M. & CASTRO, B. M. 2018. The role of remote wind forcing in the subinertial current variability in the central and northern parts of the South Brazil Bight, *Ocean Dynamics* **68**(6): 677–688.
- ETCHEVERRY, L. R., SARACENO, M., PIOLA, A. R., VALLADEAU, G. & MÖLLER, O. 2015. A comparison of the annual cycle of sea level in coastal areas from gridded satellite altimetry and tide gauges, *Continental shelf research* **92**: 87–97.

- FERNANDES, F. 2014. python-ctd v0.2.1.
URL: <https://doi.org/10.5281/zenodo.11396>
(visited on December 16th 2022)
- GARREAUD, R. 2000. Cold air incursions over subtropical South America: Mean structure and dynamics, *Monthly Weather Review* **128**(7): 2544–2559.
- GOOD, S., FIEDLER, E., MAO, C., MARTIN, M. J., MAYCOCK, A., REID, R., ROBERTS-JONES, J., SEARLE, T., WATERS, J., WHILE, J. ET AL. 2020. The current configuration of the OSTIA system for operational production of foundation sea surface temperature and ice concentration analyses, *Remote Sensing* **12**(4): 720.
- HERSBACH, H., BELL, B., BERRISFORD, P., HIRAHARA, S., HORÁNYI, A., MUÑOZ-SABATER, J., NICOLAS, J., PEUBEY, C., RADU, R., SCHEPERS, D. ET AL. 2020. The ERA5 global reanalysis, *Quarterly Journal of the Royal Meteorological Society* **146**(730): 1999–2049.
- LODER, J. W., BOICOURT, W. C. & SIMPSON, J. H. 1998. Western ocean boundary shelves coastal segment (w), *The Sea* **11**: 3–27.
- MAHIQUES, M. M. D., BURONE, L., FIGUEIRA, R. C. L., LAVENÉRE-WANDERLEY, A. A. D. O., CAPELLARI, B., ROGACHESKI, C. E., BARROSO, C. P., DOS SANTOS, S., AUGUSTO, L., CORDERO, L. M. ET AL. 2009. Anthropogenic influences in a lagoonal environment: a multiproxy approach at the Valo Grande mouth, Cananéia-Iguape system (SE Brazil), *Brazilian Journal of Oceanography* **57**(4): 325–337.
- MAMAYEV, O. I. 1975. *Temperature-salinity analysis of world ocean waters*, Elsevier.
- MARTA-ALMEIDA, M., DALBOSCO, A., FRANCO, D. & RUIZ-VILLARREAL, M. 2021. Dynamics of river plumes in the South Brazilian Bight and South Brazil, *Ocean Dynamics* **71**: 59–80.
- MCDougALL, T. J. & BARKER, P. M. 2011. Getting started with TEOS-10 and the gibbs seawater (GSW) oceanographic toolbox, *Scor/lapso WG* **127**: 1–28.
- MEISSNER, T., F. J. W. A. M. R. L. 2019. Remote sensing systems SMAP ocean surface salinities [level 2C, level 3 running 8-day, level 3 monthly], version 4.0 validated release.
URL: Available online at www.remss.com/missions/smap (visited on December 16th 2022)
- MÖLLER JR, O. O., PIOLA, A. R., FREITAS, A. C. & CAMPOS, E. J. 2008. The effects of river discharge and seasonal winds on the shelf off southeastern South America, *Continental shelf research* **28**(13): 1607–1624.
- MORAIS, P. H. L. S. 2016. *Hidrodinâmica da plataforma continental interna do estado de São Paulo*, Master's thesis, Universidade de São Paulo.
URL: <https://teses.usp.br/teses/disponiveis/21/21135/tde-24022017-181654/pt-br.php> (visited on December 16th 2022)
- PALÓCZY, A., DA SILVEIRA, I., CASTRO, B. & CALADO, L. 2014. Coastal upwelling off Cape São Tomé (22° S, Brazil): The supporting role of deep ocean processes, *Continental Shelf Research* **89**: 38–50.
- PIMENTA, F. M., CAMPOS, E. J. D., MILLER, J. L. & PIOLA, A. R. 2005. A numerical study of the Plata River plume along the southeastern South American continental shelf, *Brazilian Journal of Oceanography* **53**(3-4): 129–146.
- PIOLA, A. R., CAMPOS, E. J., MÖLLER JR, O. O., CHARO, M. & MARTINEZ, C. 2000. Subtropical shelf front off eastern South America, *Journal of Geophysical Research: Oceans* **105**(C3): 6565–6578.
- PIOLA, A. R., MATANO, R. P., PALMA, E. D., MÖLLER, O. O. & CAMPOS, E. J. 2005. The influence of the Plata River discharge on the western South Atlantic shelf, *Geophysical Research Letters* **32**(1).
- RODRIGUES, R. R. & WOOLLINGS, T. 2017. Impact of atmospheric blocking on South America in austral summer, *Journal of Climate* **30**(5): 1821–1837.

- SILVA, D. A. & DOTTORI, M. 2021. The atmospheric blocking influence over the South Brazil Bight during the 2013–2014 summer, *Regional Studies in Marine Science* **45**: 101815.
- SILVEIRA, I. C. A. D., SCHMIDT, A. C. K., CAMPOS, E. J. D., DE GODOI, S. S. & IKEDA, Y. 2000. A Corrente do Brasil ao largo da costa leste brasileira, *Rev. Bras. Ocean* **48**: 171–183.
- STARK, J. D., DONLON, C. J., MARTIN, M. J. & MCCULLOCH, M. E. 2007. OSTIA: An operational, high resolution, real time, global sea surface temperature analysis system, *Oceans 2007-europe*, IEEE, pp. 1–4.
- VALLA, D., PIOLA, A. R., MEINEN, C. S. & CAMPOS, E. 2018. Strong mixing and recirculation in the northwestern Argentine basin, *Journal of Geophysical Research: Oceans* **123**(7): 4624–4648.